UDC 621.372.22

WIDEBAND VOLUME HORN ARRAY ANTENNA WITH SWITCHABLE POLARIZATION CAPABILITY

Sergiy Y. Martynyuk, Petro Ya. Stepanenko

National Technical University of Ukraine "KPI", Kyiv, Ukraine

This paper presents the most valuable theoretical results that confirm the possibility of practical realization of a wideband volume horn array antenna with the switchable polarization capability. Among key features of the proposed antennas are their high stability of switchable linear polarization tilt angle of radiated electromagnetic wave, radiation pattern of sector type and wide operating frequency band. The paper focuses on characteristics of linear horn antenna subarrays as key components of the described volume array antenna. Subarrays fully comprise double-ridge waveguide sections. The cutoff wavenumbers calculation algorithm is developed for the symmetrical double-ridge waveguides to estimate frequency bandwidth of power dividers in their different cross sections. The problem is solved numerically by partial regions method taking into account field singularity on rectangular metal ridges.

Introduction

Numerous telecommunication systems are based on the principle of polarization diversity of electromagnetic waves [1, 2]. Fine polarization control allows reducing the polarization mismatch losses of telecommunication system and improves the overall quality of signal reception within hard active noise or under bad weather conditions. Nowadays fine polarization control is even more significant for establishing a reliable communication with versatile objects or measuring radar characteristics of hi-speed aircrafts and rockets.

As a rule, in order to build a radio communication channel with polarization control the reflector antenna with axis-symmetrical horn feed ended by polarization rotator is used [3]. The described systems of a single polarization type are characterized by significant redundancy due to the presence of free orthogonal channel for signal reception. As a result they appear to be oversized and having higher cost. One of their additional disadvantages is low frequency bandwidth that is limited by relatively narrow frequency range of single mode wave propagation of utilized circular waveguide. To broaden the working frequency range the circular waveguide can be substituted for coaxial one with azimuthally non-uniform TE_{11} mode. Frequency bandwidth expansion in this case is followed by significant complication of polarization control devices primarily dictated by the necessity to prevent excitation of fundamental transverse mode in coaxial waveguide. The best devices of this class provide the accuracy of polarization tilt angle setup around several degrees. The last appearance can cause certain instability in performance of the system with switchable polarization especially when coaxial waveguide is utilized as a key transmission line. Generally, polarization setup errors negatively influence the overall quality of communication link and for many cases cannot be acceptable.

The necessity to improve the radiating polarization characteristics of antennas makes actual the development of new principles of polarization tilt angle control. One of the possible ways to solve this complicated problem is the use of linear horn antenna subarrays with high stable slant polarizations as the basic elements of antenna system [4]. The antenna system with controlled polarization in a switchable manner can be constructed via side-by-side alignment of the radiating apertures of linear antenna subarrays consisted from appropriately inclined horns and having switchable input ports, each of which correspond to the certain discrete value of polarization tilt angle. The proposed technical solution allows obtaining high stability of antenna system polarization characteristics, moderately high gain, low insertion loss and sector type radiation pattern over wide operating frequency band.

Formulation of problem and antenna design

The objective of this paper is to investigate theoretically the possibility of practical realization of high stable antenna system with switchable polarization tilt angle by the analysis of linear in-phase horn antenna subarrays, each corresponds to a certain discrete of polarization tilt angle.

The simplest way to build the described antenna system is to combine horn antenna subarrays having different linear polarization tilt angles in one switchable electromagnetic block or otherwise in the volume horn array antenna with switchable polarization capability.Theory and technique of array antennas designed from rectangular waveguide feed and pyramidal horn

radiators are now well known and widely used in many applications [4]. Frequency bandwidth of the array antennas is strictly limited by the operating frequency range of utilized rectangular waveguide sections and commonly is not more than 40%. The use of a single ridged or symmetrical double-ridged waveguide feed instead of rectangular one, certainly, can broaden array antenna operating bandwidth since the bandwidth of the single mode propagation is broadened.

Modified in comparison to [4] linear horn antenna subarray which for the purpose of frequency bandwidth expansion up to the range 4—10 GHz utilize only double ridged waveguide sections is schematically depicted in Fig. 1. Antenna subarray principally utilizes corporate feed and consists of wideband *E*-plane double ridged waveguide power divider *2—9*, two matching sections of polarization plane rotation unit *10*, *11* and double ridged flare angle horn radiators with rectangular apertures *12*.

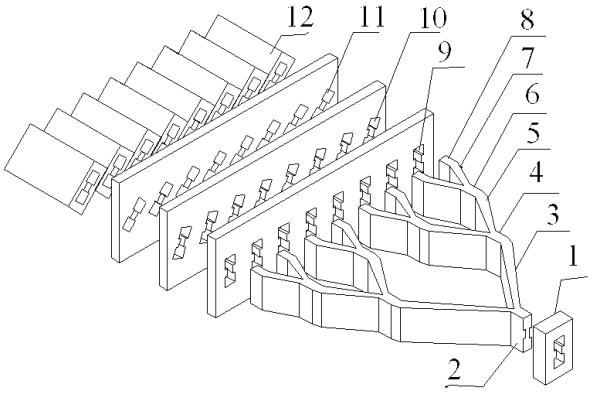

Fig. 1. Schematic illustration of modified linear horn array antenna of inclined polarization: (*1*) double ridge waveguide output of mode transducer from coaxial line; (*2*) input double ridge waveguide of the eight-way power divider; (*3*,*5*,*7*) two-way power dividers; (*4*,*6*) nearly quarter-wave transformer piece of double ridge waveguide between cascades of whole power divider; (*8*) output double ridge waveguide of the eight-way power divider; (*9*) nearly quarter-wave transformer piece of double ridge waveguide between divider output and input of polarization plane rotation unit; (*10*) the first matching section of polarization plane rotation unit in the form of double ridge waveguide; (*11*) the second matching section of polarization plane rotation unit; (*12*) inclined horn radiators.

Each radiator of the array is a symmetrical double-ridged horn with rectangular aperture that contains smooth transition between a symmetrical double ridged waveguide to a pyramidal horn. This transition is designed in such a manner that the sizes of the double ridged waveguide cross-section (width, height and gap between ridges) are continuously increased from the horn input to the radiating aperture. A flare angle of horn radiators was selected relatively small in order to provide the possibility of compact packaging of radiators in array and to obtain required parameters of sector type radiation patterns in horizontal and vertical planes in the whole frequency band. Horn radiators have inclined orientation in order to achieve required value of linear polarization tilt angle of radiated electromagnetic wave. They are arranged closely to each other to minimize sidelobe level in array plane of radiation pattern.

Mismatching of horn radiators is mostly caused by reflection from the boundary between the rectangular waveguide aperture and free space. Generally, a level of these reflections increases at the lower end of operating frequency range. The electromagnetic waves reflected from free space boundary interfere with waves generated on internal horn discontinuities and with waves caused by electromagnetic coupling between horn radiators in subarray. Following the purpose to achieve high subarray performance the design of ridged horn profile should be optimized to provide low levels of active VSWR (less than 1.5) over frequency band 4—10 GHz for the majority of horn radiators. Our additional investigations show that formulated above condition can be fulfilled for the total length of horn in the order of 180 mm.

An excitation of every subarray is carried out by *E*-plane double ridged waveguide power divider typically constructed from a number of two-way symmetrical dividers fully based on double ridged waveguide sections and connected by short joint sections. The overall power divider defines the amplitude and phase relations of electromagnetic fields at the horn apertures. Lengths of joint sections are selected to achieve good amplitude balance (better 0.05 dB) at the outputs of power dividers and provide good matching.

One or two sections of polarization rotation unit are necessary to organize well-matched stepped polarization transformation from linear horizontal (see Fig. 1) to required linear inclined type. Note that only one section in polarization rotating unit is good enough for polarization tilt angles less than 20° related to the plane of subarray.

To achieve higher polarization tilt angle, for example close to 60° related to the plane of array polarization, rotation unit was designed on the base of two short doubled-ridged waveguide sections (also with single mode propagation) rotated around their symmetry planes by 30º comparing with output symmetrical double ridged waveguide sections of power divider. Length of each polarization rotation section in proposed design is equal to 13 mm or approximately quarter of wavelength for the central operating frequency. This subarray antenna provides a broad band operation when

the purely fundamental mode propagation from the antenna input to its radiator over wide frequency band is established. This condition can be implemented by using a broadband double ridged waveguide transmission line everywhere at the antenna design.

A design feature of the wide-band power divider assumes the necessity to control the cross-sections dimensions of the double-ridged waveguide in order to avoid the discharge over range of single-mode regime. This situation specifies the necessity of rigorous computation of the cutoff frequencies for the fundamental mode and for the first higher order transverse-electric and transverse-magnetic modes.

Mathematical models of double-ridged waveguide

One-quarter part of the cross-section of the considered symmetrical double-ridged waveguide is shown in Fig. 2. A task is solved in assumption that metallic walls of the waveguide have an ideal conductivity. We suppose that there is a magnetic wall in vertical symmetry plane of the waveguide and an electric wall in horizontal symmetry plane.

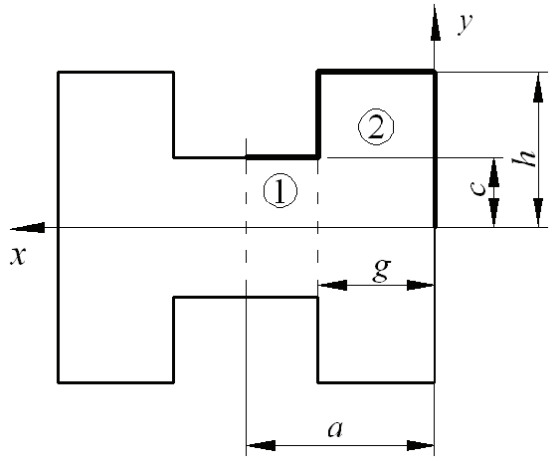

Fig. 2. Double-ridged waveguide cross-section.

We solve the tasks for transverse-electric and transverse-magnetic modes by the partial region method with taking into account the edge field singularity [5]. According to [5] the solution of Helmholz's equation for transverse-electric modes in partial regions 1 and 2 can be written as follows

$$\psi_1 = \sum_m A_m \sin\alpha_m(a-x)\cos p_m y; \qquad (1)$$

$$\psi_2 = \sum_m B_m \cos\beta_m x \cos q_m y, \qquad (2)$$

where $\alpha_m = (\kappa_\mu^2 - p_m^2)^\varphi$; $\beta_m = (\kappa_\mu^2 - q_m^2)^\varphi$; $p_m = m\pi/c$; $q_m = m\pi/h$; κ_μ is the cutoff wavenumber for μ th mode; ψ_1, ψ_2 are components of scalar eigenfunction of double ridged waveguide; A_m and B_m are the unknown coefficients; $m = 0,1,2,...,M_1 - 1$ for region 1; M_1 is the number of terms in series (1); $m = 0,1,2,...,M_2 - 1$ for region 2; M_2 is number of terms in series (2); $\varphi = 1/2$.

The unknown coefficients in (1) and (2) can be found through the electric field value on the common boundary of partial regions. Defining the electric field on the boundary as $E_y = -d\psi_1/dx$; $E_y = -d\psi_2/dx$ and taking into account the orthogonality conditions of the functions $\cos p_m y$; $\cos q_m y$ on the intervals c, h respectively, one can obtain the following expressions for the unknown coefficients:

$$A_m = 2\varepsilon_m/(c\alpha_m\cos\alpha_m b)\int_0^c E_y \cos p_m y dy; \qquad (3)$$

$$B_m = 2\varepsilon_m/(h\beta_m\sin\beta_m g)\int_0^c E_y \cos q_m y dy, \qquad (4)$$

where $b = a - g$; $\varepsilon_m = 1/2$ if $m = 0$ otherwise $\varepsilon_m = 1$.

By substituting (3), (4) into expressions (1), (2) and equating the resultant magnetic fields on the common boundary of partial regions one can obtain the integral equation relatively to tangential electric field in coupling window [5]. To solve this integral equation it is proposed to approximate the unknown electric field in coupling window by series of Gegenbauer's polynomials [5]. By substituting this expression for the approximate electric field into integral equation and using Galerkin's method, we obtain the following homogeneous system of linear algebraic equations:

$$\sum_i X_i\Big[\sum_m 2U_i U_j \varepsilon_m/\alpha_m \tan\alpha_m b - \sum_m 2V_i V_j c/h\varepsilon_m/\beta_m \cot\beta_m g\Big] = 0; \qquad (5)$$

$$U_i = (-1)^i \pi\Gamma(2i+2\lambda)J_{2i+\lambda}(m\pi)/[(2i)!\Gamma(\lambda)(2m\pi)^\lambda];$$

$$V_i = (-1)^i \pi\Gamma(2i+2\lambda)J_{2i+\lambda}(q_m c)/[(2i)!\Gamma(\lambda)(2q_m c)^\lambda].$$

Here $\lambda = 1/6$; $\Gamma(2i+2\lambda)$, $\Gamma(\lambda)$ are the gamma functions; $J_{2i+\lambda}(m\pi)$, $J_{2i+\lambda}(q_m c)$ are the Bessel's functions of the first kind; X_i are the unknown expansion coefficients of the electric field in coupling window; $i = 0,1,...,I-1$; $j = 0,1,...,I-1$; I is the number of expansion terms; U_j, V_j quantities are obtained from U_i, V_i by replacement of indexes.

A condition of nontrivial solution of (5) is equality to zero of its determinant. This equality represents the characteristic equation for computing the cutoff wavenumbers of transverse-electric modes of double-ridged waveguide. As follows from (5), the cutoff wavenumbers implicitly enter this system. This means

that determinant of the system (5) is the transcendental function of κ. Hence, an estimation of cutoff wavenumbers κ_μ should be carried out by consecutive finding of determinant zeros. The consecutive approach methods can be employed to solve this problem.

We utilize the dichotomy method to find the determinant zeros. This method is based on the sign estimation of function under consideration on the both ends of interval along wavenumbers axis. As can be seen from (5) the investigated function contains breaks besides zeros. The determinant of system (5) has the different signs on the both sides of breaks point. Hence this point will be perceived by program as the cutoff wavenumber that is knowingly in error.

To avoid such errors the mentioned points should be excluded from the consideration. The location of these points on the wavenumber axis can be defined by solving of the following equations:

$$\cos\alpha_m b = 0;\ \sin\beta_m g = 0.$$

By performing the necessary transformation, we obtain

$$\kappa = [(u\pi / b)^2 + (v\pi / c)^2]^{\varphi};$$
$$\kappa = [(u\pi / g)^2 + (v\pi / h)^2]^{\varphi}, \quad (6)$$

where $u = 0,1,2,...;\ v = 0,1,2,....$

The computed results indicate that the zeros and breaks of the determinant can be very close. Hence at the computer realization of the dichotomy method, the bypass of breaks points through using expressions (6) yet not ensure an absence of spurious roots of dispersive equation.

To significantly increase the computer algorithm reliability at the calculation of higher modes we use a functional for cutoff numbers [6] which in considered case takes the form:

$$\kappa_\mu^2 = \int_s (\mathrm{grad}\psi_\mu)^2 ds / \int_s \psi_\mu^2 ds, \quad (7)$$

where ψ_μ is the μth mode scalar eigenfunction of the double ridged waveguide; s denotes the square of its cross-section.

The equality (7) is fulfilled if and only if κ will be the cutoff wavenumber, that is $\kappa = \kappa_\mu$. To apply the expression (7) to calculation algorithm of the cutoff wavenumbers of double-ridged waveguide we should define the transversal components of the overall fields in accordance with differential operator:

$$-\mathbf{z} \times \mathbf{u}\mathrm{grad}\psi = -\mathbf{y}\partial\psi / \partial x + \mathbf{x}\partial\psi / \partial y, \quad (8)$$

where $\mathbf{u}$ is an unity vector; $\mathbf{x}$, $\mathbf{y}$, $\mathbf{z}$ are the unity vectors directed along x, y and z axes respectively.

To perform the computations in accordance with (8) it is necessary to solve the homogeneous system of linear algebraic equations. As a result the unknown coefficients X_i and the distribution of tangential components of electrical fields in coupling window for various transverse-electric modes will be obtained. To solve the system (5) we suppose that the first coefficient of approximating series is equal to unity. By excluding the first equation of (5) and shifting the resulting column of flexible terms into right part we obtain the non-uniform system of linear algebraic equations for calculating the remaining coefficients.

At the computation of the coefficients under unknowns it is necessary to determine Bessel's functions of fractional indexes $\lambda = 1/6 + 2i$, where i is the same as in (5). An algorithm of this functions estimation based on recursive procedure operating in direction from high indexes to small ones was developed. This algorithm allows achieving a high accuracy of the Bessel's function computation. In fact, this accuracy is defined entirely by capability of computer used.

As the unknown coefficients X_i and the distribution of tangential components of electrical fields in coupling window for various transverse-electric modes have been obtained the amplitude coefficients in (3) and (4) acquire the following form:

$$A_m = 2\varepsilon_m \delta_m / (\alpha_m \cos\alpha_m b); \quad (9)$$

$$B_m = 2\varepsilon_m c\sigma_m / (h\beta_m \sin\beta_m g); \quad (10)$$

$$\delta_m = \sum_i X_i U_i;\ \sigma_m = \sum_i X_i V_i.$$

To compute the denominator in (7) we use (1), (2) and evaluation ranges of those functions for every mode. Considering as before only one-quarter part of the cross-section of the symmetrical double-ridged waveguide and taking into account the orthogonality conditions of the functions $\cos p_m y$, $\cos q_m y$ on the intervals c and h respectively we obtain

$$\int_s \psi_\mu^2 ds = \sum_m A_m^2 \int_s (\sin\alpha_m b)^2 ds + \sum_m B_m^2 \int_s (\cos\beta_m x)^2 ds$$

where the coefficients A_m, B_m are evaluated by expressions (9), (10).

When integrals in this formula are calculated we obtain the following expression for the denominator in (7):

$$\int_s \psi_\mu^2 ds = \sum_m 2\varepsilon_m bc\delta_m^2 / \alpha_m^2 \times$$
$$\times[1/(\cos\alpha_m b)^2 - (\tan\alpha_m b)/(\alpha_m b)] +$$

$$+\sum_m 2\varepsilon_m g c^2 \sigma_m^2 / (h\beta_m^2) \times$$
$$\times[1/(\sin\beta_m g)^2 + (\cot\beta_m g)/(\beta_m g)]. \quad (11)$$

To determine the numerator in (7) it is necessary to find the components (8) in partial regions. By substituting in (8) the expressions for scalar eigenfunctions components of double-ridged waveguide (1) and (2) we obtain

$$-\mathbf{z}\times\mathbf{u}\,\mathrm{grad}\psi_1 = \mathbf{y}\sum_m A_m\alpha_m\cos\alpha_m(a-x)\cos p_m y -$$
$$-\mathbf{x}\sum_m A_m p_m \sin\alpha_m(a-x)\sin p_m y; \quad (12)$$
$$-\mathbf{z}\times\mathbf{u}\,\mathrm{grad}\psi_2 = \mathbf{y}\sum_m B_m\beta_m \sin\beta_m x\cos q_m y -$$
$$-\mathbf{x}\sum_m B_m q_m \cos\beta_m x\sin q_m y. \quad (13)$$

Combining (12), (13) and evaluating the integrals we get

$$\int_s (\mathrm{grad}\psi_\mu)^2 ds = \sum_m 2\varepsilon_m bc\delta_m^2/\alpha_m^2 \times$$
$$\times[(\alpha_m^2+p_m^2)/(\cos\alpha_m b)^2 + (\alpha_m^2 - p_m^2)(\tan\alpha_m b)/(\alpha_m b)] +$$
$$+\sum_m 2\varepsilon_m g c^2\sigma_m^2/(h\beta_m^2)[(q_m^2+\beta_m^2)/(\sin\beta_m g)^2 +$$
$$+(q_m^2-\beta_m^2)(\cot\beta_m g)/(\beta_m g)]. \quad (14)$$

If $\kappa_\mu^2 - p_m^2 < 0$ or $\kappa_\mu^2 - q_m^2 < 0$, the corresponding trigonometric functions in expressions (13) and (14) should be replaced by hyperbolic ones. Despite the presence of imaginary components in (13) and (14), their overall values are always real.

Consider briefly the computational algorithm for finding cutoff wavenumbers of transverse-magnetic modes based on technique [5]. According to [5] scalar eigenfunctions of partial regions can be written as follows

$$\xi_1 = \sum_n A_n \cos\alpha_n(a-x)\sin p_n y; \quad (15)$$
$$\xi_2 = \sum_n B_n \sin\beta_n x \sin q_n y. \quad (16)$$

where $\alpha_n = (\varsigma_\nu^2 - p_n^2)^\varphi$; $\beta_n = (\varsigma_\nu^2 - q_n^2)^\varphi$; $p_n = n\pi/c$; $q_n = n\pi/h$; ς_ν is the cutoff wavenumber for ν th mode; A_n and B_n are the unknown coefficients; $n = 1,2,...,N_1$ for region 1; N_1 is the number of terms in series (15); $n = 1,2,...,N_2$ for region 2; N_2 is number of terms in series (16).

Similar to the previous case in [5] the integral equation with respect to tangential electric field in coupling window was obtained. The solution of this integral equation by the Galerkin's method leads to the following homogeneous system of linear algebraic equations relatively to unknown expansion coefficients of tangential electric field

$$\sum_i X_i[\sum_n 2U_i U_j \alpha_n \tan\alpha_n b - \sum_n 2V_i V_j c/h\beta_n \cot\beta_n g] = 0;$$
$$U_i = (-1)^i \pi[\Gamma(\tau)J_\zeta(n\pi)]/[(2i+1)!\Gamma(\vartheta)(2n\pi)^\vartheta];$$
$$V_i = (-1)^i \pi[\Gamma(\tau)J_\zeta(q_n c)]/[(2i+1)!\Gamma(\vartheta)(2q_n c)^\vartheta]. \quad (17)$$

Here $\tau = 2i + 2\vartheta + 1$; $\zeta = 2i + \vartheta + 1$; $\vartheta = 7/6$; $\Gamma(\tau)$, $\Gamma(\vartheta)$ are the gamma functions; $J_\zeta(n\pi)$, $J_\zeta(q_n c)$ are the Bessel's functions of the first kind; X_i are the expansion coefficients of the electric field in coupling window; $i = 0,1,...,I-1$; $j = 0,1,...,I-1$; I is the number of expansion terms; U_j, V_j quantities are obtained from U_i, V_i by replacement of indexes.

The resolution algorithm of system (17) is the same as (5). The points on the wavenumber axis in which there are breaks of determinant of (17) and which should be excluded from the calculation we can define by solving of the following equations:

$$\cos\alpha_n b = 0;\ \sin\beta_n g = 0.$$

Resolution of these equations provides the following values of wavenumbers:

$$\varsigma = [(u\pi/b)^2 + (v\pi/c)^2]^\varphi;$$
$$\varsigma = [(u\pi/g)^2 + (v\pi/h)^2]^\varphi,$$

where $u = 0,1,2,...$; $v = 1,2,...$.

As the unknown coefficients X_i have been found from solution (17) and the distribution of tangential components of electrical fields in coupling window for various transverse-magnetic modes have been obtained the amplitude coefficients in (15) and (16) get the form:

$$A_n = 2\delta_n/\cos\alpha_n b; \quad (18)$$
$$B_n = 2c\sigma_n/(h\sin\beta_n g); \quad (19)$$
$$\delta_n = \sum_i X_i U_i;\ \sigma_n = \sum_i X_i V_i,$$

where the values U_i and V_i are determinate by expressions (17).

Consider a sequence of calculation associated with the use of the functional for cutoff wavenumbers [6] which in the case of transverse-magnetic modes takes the form

$$\varsigma_\nu^2 = \int_s (\mathrm{grad}\xi_\nu)^2 ds / \int_s \xi_\nu^2 ds, \quad (20)$$

where ξ_ν represents the ν th mode scalar eigenfunction of the double ridged waveguide; s is the square of waveguide cross-section.

Likewise to (7) equality (20) is fulfilled if and only if ς will be the cutoff wavenumber of transverse-magnetic mode, that is $\varsigma = \varsigma_\nu$. As in the previous case, for application of the expression (20) to calculation algorithm of the cutoff wavenumbers of double-ridged waveguide we should define the transversal components of the overall fields in accordance with differential operator:

$$\mathbf{u}\,\mathrm{grad}\xi = \mathbf{x}\partial\xi / \partial x + \mathbf{y}\partial\xi / \partial y, \qquad (21)$$

where $\mathbf{u}$, $\mathbf{x}$, $\mathbf{y}$ are the unity vectors the same as in expression (8).

According to (21), we obtain the following expression for transversal components of the electric fields:

$$\mathbf{u}\,\mathrm{grad}\xi_1 = \mathbf{x}\sum_n A_n\alpha_n \sin\alpha_n(a-x)\sin p_n y + \\ +\mathbf{y}\sum_n A_n p_n \cos\alpha_n(a-x)\cos p_n y; \qquad (22)$$

$$\mathbf{u}\,\mathrm{grad}\xi_2 = \mathbf{x}\sum_n B_n\beta_n \cos\beta_n x \sin q_n y + \\ +\mathbf{y}\sum_n B_n q_n \sin\beta_n x \cos q_n y. \qquad (23)$$

Using (15), (16) and evaluating the integrals similarly to previous consideration, we obtain

$$\int_s \xi_\nu^2 ds = \sum_n 2bc\delta_n^2 \times \\ \times[1/(\cos\alpha_n b)^2 + (\tan\alpha_n b)/(\alpha_n b)] + \\ +\sum_n 2gc^2\sigma_n^2 / h \times \\ \times[1/(\sin\beta_n g)^2 - (\cot\beta_n g)/(\beta_n g)]. \qquad (24)$$

Combining (22), (23) and evaluating the integrals we get

$$\int_s (\mathrm{grad}\xi_\nu)^2 ds = \sum_n 2bc\delta_n^2 \times \\ \times[(p_n^2+\alpha_n^2)/(\cos\alpha_n b)^2 + (p_n^2-\alpha_n^2)(\tan\alpha_n b)/(\alpha_n b)] + \\ +\sum_n 2gc^2\sigma_n^2 / h[(\beta_n^2+q_n^2)/(\sin\beta_n g)^2 + \\ +(\beta_n^2-q_n^2)(\cot\beta_n g)/(\beta_n g)]. \qquad (25)$$

As well as in (13), (14) if $\varsigma_\nu^2 - p_n^2 < 0$ or $\varsigma_\nu^2 - q_n^2 < 0$, the corresponding trigonometric functions in expressions (24) and (25) should be replaced by hyperbolic ones. Despite the presence of imaginary components in (24) and (25), their overall values are always real.

According to received relations the computation of the cutoff frequencies were carried out for fundamental mode and first higher transverse-electric and transverse-magnetic modes. On the bases of computed results the evaluation of broadband properties of the double-ridged waveguide were investigated in wide range of its cross-section parameters. The theoretical results obtained were applied for designing of power divider.

To illustrate the algorithm operation we consider the case when normalized dimensions of double ridged waveguide cross-section are $h/a = 0.5$; $g/a = 0.6$; $c/h = 0.5$. According to [5], in this case the normalized values of cutoff wavenumbers of fundamental mode and the first higher transverse-magnetic mode are $\kappa_1 a = 1.1790$ and $\varsigma_1 a = 8.0485$ respectively.

At the computations, the numbers of expansion terms in series (1), (2) were chosen in accordance with a rule $M_1 / M_2 = c/h$ where $M_1 = 400$; $M_2 = 800$. The corresponding relation for expressions (15), (16) is $N_1 / N_2 = c/h$ with $N_1 = 400$; $N_2 = 800$.

To find the expansion coefficients of electrical fields on the common boundary of partial regions 1 and 2 for both transverse-electric and transverse-magnetic modes the systems (5) and (17) each of the fourth order were solved. For computation of the Bessel's functions with high accuracy by the recursive procedure about 1500 iterations was used. An examination of this procedure showed that the calculation accuracy of Bessel's functions of fractional indexes achieves 10—12 true decimal symbols.

According to the computations the following numerical values of normalized cutoff wavenumbers were obtained for first two transverse-electric modes and one first higher transverse-magnetic mode: $\kappa_1 a = 1.1789506143184965$; $\kappa_2 a = 4.8514066169966217$ and $\varsigma_1 a = 8.0483338641326299$ respectively. The calculation by using expressions (7) and (20) gives the following values of normalized cutoff wavenumbers: $\kappa_1 a = 1.178950614318501$; $\kappa_2 a = 4.851406616996620$ and $\varsigma_1 a = 8.0483338641326387$. A comparison of these results indicates that expressions (7) and (20) with high accuracy reproduce the values of cutoff wavenumbers for both types of electromagnetic waves.

Suppose now that on the wavenumber axis there are the points corresponding to breaks of determinants of the system of linear algebraic equations (5) or (17). Let their values are equal to $\kappa_{1s} a = 2$; $\kappa_{2s} a = 4$; $\varsigma_{1s} a = 8.5$ and they are perceived by the program as the roots of the given determinants. These spurious roots are used for evaluation of functionals (7) or (20). As a result we get $\kappa_{1f} a = 3.016\,3$; $\kappa_{2f} = 3.92$; $\varsigma_{1f} = 9.43$. It follows from this illustration that in the case of spurious cutoff wavenumbers the values κ_{1s}; κ_{2s}; ς_{1s} significantly dif-

fer from the calculated ones κ_{1f}; κ_{2f}; ς_{1f}. Thus the designing technique proposed ensures an absence of spurious solutions in a large number of the double-ridged waveguide problems.

This designing technique was applied to estimation of the broadband properties of the symmetrical double-ridged waveguide in the compound structure of the power divider which is used for excitation of horn subarray antenna. We carried out the computation of the cross-section dimensions of the double-ridged waveguide which ensure near constant of the cutoff frequency of fundamental mode under its propagation along the power divider channels. The second demand for the estimation of this dimensions was the necessity to provide the bandwidth which is sufficient for power divider operation under conditions when it is originated no higher modes along all the way of the electromagnetic wave propagation.

For ability illustration of the algorithm proposed in the following figures the calculated results of overlapping in frequency γ are presented for wide range variation of double ridged waveguide cross-section dimensions. The quantity of γ is represented as the minority among the calculated values of $\gamma_1 = \kappa_2 / \kappa_1$ and $\gamma_2 = \varsigma_1 / \kappa_1$ for every waveguide parameter.

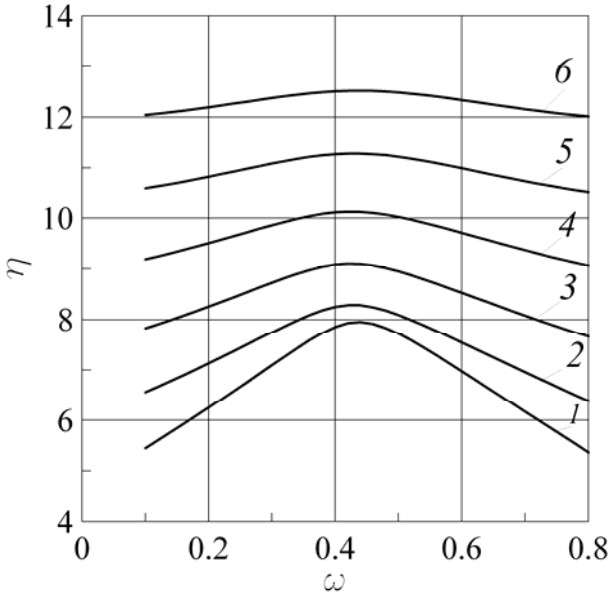

Fig. 3. Frequency overlapping band versus relative ridge width for various values of normalized gap between ridges.

Fig. 3 illustrates the normalized frequency overlapping band $\eta = \gamma + 1.5\rho$ as a function of ridge relative width $\omega = b / a$ for various values of normalized gap between ridges $c / h = 0.2 + 0.1(\rho - 1)$, where ρ is the curvature number.

It can be seen from Fig. 3 that the value of frequency overlapping band γ slightly depends on the ridge width. As follows from represented curvatures the maximum values of γ are located in the middle range of relative ridge width variations. Due to the slight dependence of γ as a function of the value ω the ridge width can be chosen from manufactory considerations.

Fig. 4 illustrates the normalized frequency overlapping band $\eta = \gamma + \rho$ where ρ is the curvature number as a function of relative gap between ridges $\chi = c / h$ for various values of width ridge to width waveguide ratio $\omega = b / a = 0.1\rho$.

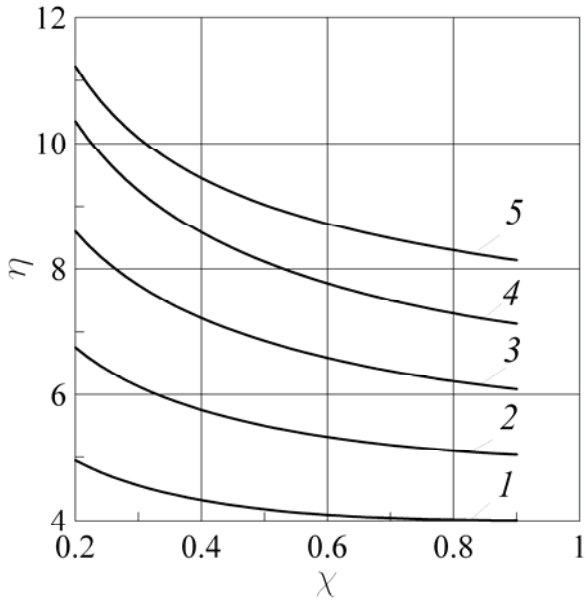

Fig. 4. Frequency overlapping band as a function of relative gap between ridges for various values of width ridge to width waveguide ratio $\omega = b / a$.

It should be noted, that the present analysis was carried out in assumption of ideal symmetry of double-ridged waveguide cross-section and perfect manufacture of power divider. However, a manufacturing inaccuracy of prototypes always takes place in practice. Therefore the real values of frequency overlapping band may be significantly low because of higher modes excitation on the discontinuities of junctions.

Results

The linear antenna subarrays consisting of 16 inclined horns was optimized for various inclination angles of radiators in the range from 30° to 60° with a step 5°. Waveguide cross-sections were controlled by algorithm described in the above section in order to establish single fundamental mode propagation for all frequencies from 4 to 10 GHz. Optimal geometries of all waveguide components of the array antenna were ob-

tained via numerical calculations using finite-difference time-domain and finite-element methods. Each horn radiator had length 180 mm, aperture sizes 46×30 mm and thickness of metal wall 2 mm. Inclined horns were arranged in linear subarray in vertical plane periodically at a minimum possible distance to provide the absence of air gaps between them. Thus, the subarray period was changed from 40 mm to 62 mm in order to get the horn inclination angles raising from 30° to 60°. Numerically examined subarrays provide sector type radiation pattern for all operating frequencies. Fig. 5 shows a typical calculated radiation pattern in the principal planes for the 16-element vertically oriented linear subarray with the horn inclination angle 45° for 6 GHz frequency. A gain factor of this horn antenna subarray increase with frequency as depicted in Fig. 6.

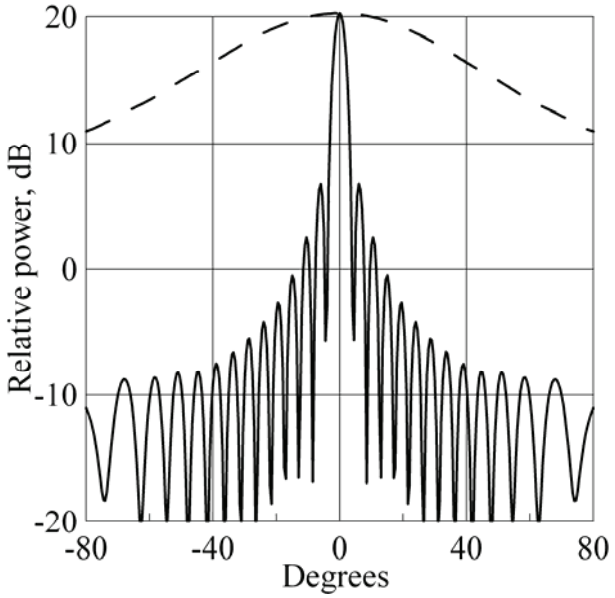

Fig. 5. Calculated radiation pattern of 16-element horn array with linear polarization angle 45° at frequency 6 GHz: vertical plane (solid line); horizontal plane (dashed line).

It is well known, that pure and predictable polarization characteristics in wide frequency band can be achieved only in case of ideally symmetrical antenna structures. However, the asymmetry of subarray composed from inclined horn radiators may cause certain undesirable depolarization effect. Our calculations show that the resulting polarization of radiated electromagnetic wave remain almost linear inside 6 dB sector of radiation pattern but its tilt angle is not exactly equal to the rotation angle of horns in subarray. Moreover the resultant polarization tilt angle is frequency and direction sensitive. Fig. 7 presents polarization tilt angle characteristics versus frequency for standalone linear subarrays composed from 16 horns inclined to 40°, 45°, 50° and 60° respectively. In Fig. 7 only broadside (main) direction of radiation is considered. Obviously, polarization tilt angle even for the main direction of radiation can vary approximately within ±3° comparing to the rotation angle of horns.

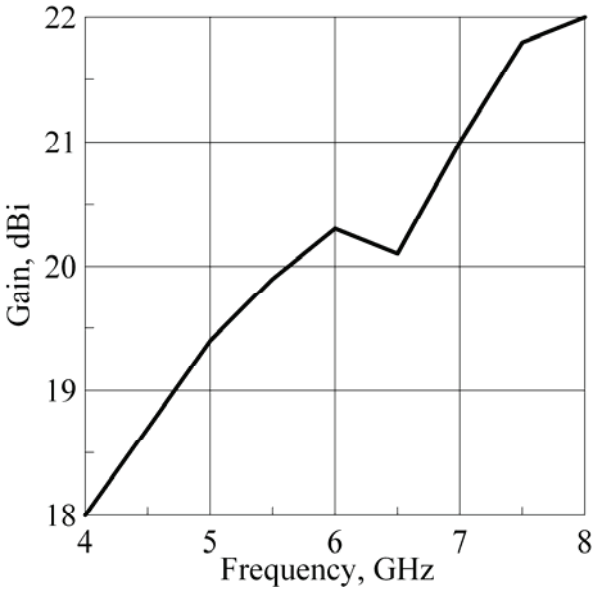

Fig. 6. Calculated gain of 16-element horn array.

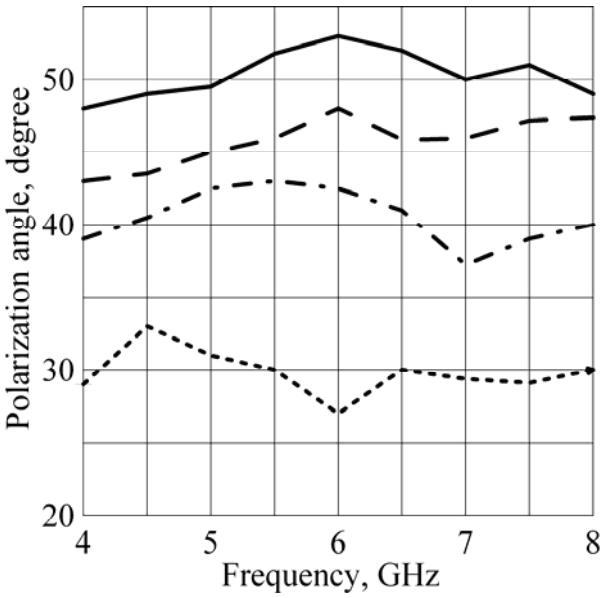

Fig. 7. Linear polarization angle in the main direction of radiation versus frequency for different rotation angles of horns in array: $\theta = 40^{\circ}$ (solid line); $\theta = 45^{\circ}$ (dashed line); $\theta = 50^{\circ}$ (dashed-dotted line); $\theta = 60^{\circ}$ (dotted line).

Fig. 8 shows changing of polarization tilt angle inside horizontal sector of radiation pattern for optimized subarray having inclined to 45° horns. Polarization tilt angle in all curves decrease when observing angle of radiation pattern increase. In this case an observer located in the far zone sees cosine projection of the horn

apertures. Described cosine effect should be taken into account if it is necessary to control the stable value of polarization tilt angle not only along one direction but inside the wide sector. For example such task can arise in modern radar applications.

The characteristics obtained prove the fact, that wideband subarray composed from rotated horns can be realized for a number of linear inclined polarization angles. To achieve the required value of polarization tilt angle of radiated field in the far zone, the horn rotation angle need to be adjusted. To this end, we can propose the following iterative procedure. Initially one need to obtain the polarization characteristics for linear subarray of equally excited horns rotated on the angle equal to the required value of polarization tilt angle. After estimating of resulting polarization tilt angle error the rotation angle of horns should be corrected to the value which is mathematically equal to the detected error. Specified procedure can be repeated several times to rich proper polarization characteristics.

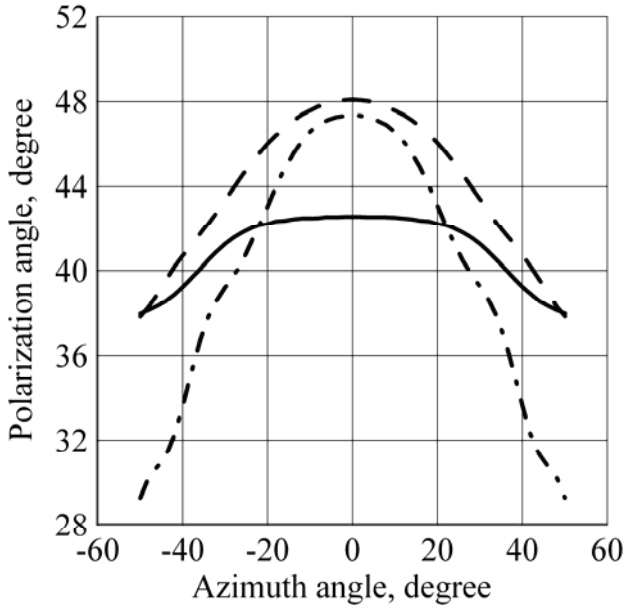

Fig. 8. Linear polarization angle in horizontal plane for rotation angle of horns in array $\theta = 45^{\circ}$: $f = 4$ (solid line); $f = 6$ (dashed line); $f = 8$ (dashed-dotted line).

A volume horn array antenna is consisted from several linear subarrays according to the number of polarization tilt angle discrete. Inputs of subarrays are supposed to be switchable and thus disposed as close as possible one to each other. It means that subarrays apertures occur to be also closely located and consequently a mutual coupling between subarrays may significantly influence the polarization characteristics of the system. Fig 9 shows a calculated mutual coupling coefficient between central and neighboring inclined horns in subarray for the rotational angle 45°. Significant level of mutual coupling (more than -25 dB) is identified only for the nearest horns in subarray for the lower frequencies of operating band.

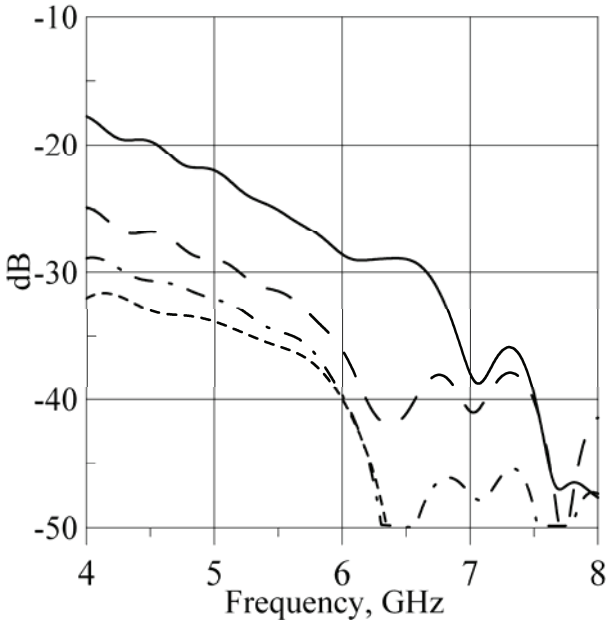

Fig. 9. Coupling between horns in 16-element subarray antenna: 8—9 (solid line); 8—10 (dashed line); 8—11 (dashed-dotted line); 8—12 (dotted line).

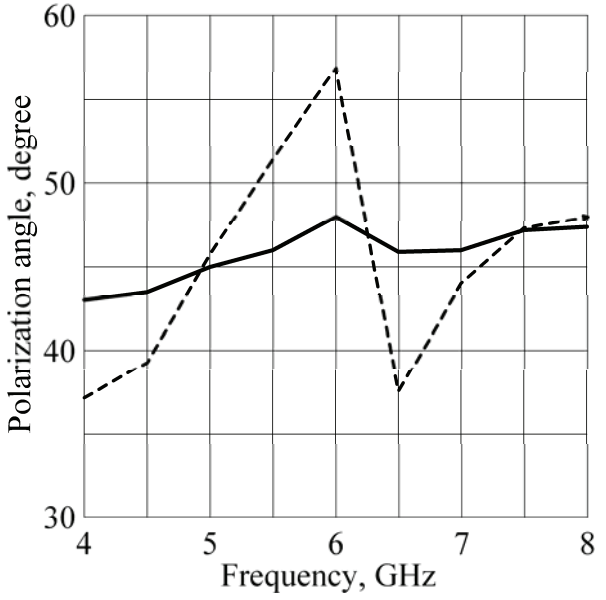

Fig.10. Polarization tilt angle of 16-element subarray: case of standalone subarray (solid line); case of two closely disposed subarrays with horns rotated to –45° and +45° (dashed line).

Additional investigations show that mutual coupling effects between subarrays can be ignored for the case of vertical alignment of vertically oriented linear subarrays of horns in switchable system. For the case of their side by side alignment in horizontal plane one should be more careful. Fig. 10 demonstrates polarization tilt an-

gle value in main direction versus frequency for the case when two 16-element subarrays having horns rotated to $-45°$ and $+45°$ respectively are positioned at a distance 62 mm between centers of horn apertures (1 mm between metal corners of horns) in horizontal plane.For this critical case resulting polarization tilt angle error due to mutual coupling effect can vary up to $\pm 10°$ comparing to standalone case for certain frequency points. It should be noted, the errors occurred during polarization setup inside 6 dB sector of radiation pattern due to mutual coupling between subarrays can be ignored if metal corners of the horns separate at a distances more than two wavelengths.

Conclusion

The simplest way to build the wideband volume horn array antenna with the switchable polarization capability is to combine horn antenna subarrays having different linear polarization tilt angles in one switchable electromagnetic block. The possibility of wideband linear polarization control in a switchable manner is shown and design of volume horn array antenna is presented. This antenna contains a set of linear antenna subarrays composed from 16 inclined horns. Inclined horns in subarrays are cophased and equiamplitude excited by *E*-plane wideband power divider loaded by polarization rotators.

A key feature of subarray design is the utilization only double-ridged waveguide sections and providing single fundamental mode propagation from antenna input to the apertures over wide frequency band. The use of the symmetrical double-ridge waveguide feed instead of rectangular one can certainly broaden array antenna operating bandwidth since the bandwidth of the single mode propagation is broadened.

Optimization of geometric parameters of ridged horns was performed using successive approximation method to provide their operation over wide frequency band. This ensures single mode wave propagation and cutoff frequencies to be approximately equal along a ridged waveguide in order to minimize return losses of ridged waveguide power dividers. The cutoff wavenumbers calculation algorithm is developed for the symmetrical double-ridge waveguides to estimate frequency bandwidth of power dividers in their different cross sections.

The algorithm for computing of cutoff wavenumbers of symmetrical double ridged waveguides is based on rigorous solution of Helmholz's equation for transverse-electric and transverse-magnetic modes. The problem was solved numerically by partial regions technique taking into account field singularity on rectangular metal ridges. The stability of developed algorithm was increased by implementation of functionals in description of waveguide cutoff wavenumbers. For calculation of these functionals, the all components of electromagnetic fields in double-ridged waveguide have been determined. The computed results show that the designing technique proposed ensures an absence of spurious solutions in a large number of the double-ridge waveguide problems.

The radiation and polarization characteristics of linear horn antenna subarrays are theoretically investigated and discussed. The calculated polarization characteristics show that asymmetry in geometry of standalone linear subarray composed from inclined horns leads to an error between the resulting polarization tilt angle of electromagnetic wave in the far zone and inclination angle of ridged horns in subarray. This error depends on the frequency and the observation direction in the far zone. The procedure that allows adjust the inclination angle of horns in appropriate linear subarray is presented. It was shown that mutual coupling between horn antenna subarrays arranged side by side in volume array antenna can make negative impact on the polarization characteristics inside 6 dB sector of subarray radiation pattern, if distance between metal edges of subarrays appears to be less than two wavelengths.

References

1. Characterization of polarization diversity at the mobile / T. W. C. Brown, S. R. Saunders, S. Stavrou, M. Fiacco // IEEE Transactions on Vehicular Technology. — 2007. — Vol. 56, N. 5. — P. 2440—2447.

2. Dual-polarized wireless communications: from propagation models to system performance evaluation / C. Oestges, B. Clerckx, M. Guillaud, M. Debbah // IEEE Transactions on Wireless Communications. — 2008. — Vol. 7, N. 10. — P. 4019—4031.

3. Wide-band linearly or circularly polarized monopulse tracking corrugated horn / B. Du, E. K. N. Yung, K. Z. Yang, W. J. Zhang // IEEE Transactions on Antennas and Propagation. — 2002. — Vol. 50, N. 2. — P. 192—197.

4. Ultra wideband linear horn array antenna with slant polarization / F. F. Dubrovka, S. Y. Martynyuk, V. V. Marchenko, P. Ya. Stepanenko at al. // Proceedings of International Conference on Antenna Theory and Techniques, May 24—27, 2005, Kyiv, Ukraine. — P. 283—286.

5. Waveguides with complicated cross-sections / G. F. Zargano, V. P. Lapin, V. S. Mikhalevskiy, at al. – Moscow: Radio and Communication, 1986. — 124 p. [in Russian].

6. Morse P. M., Feshbach H. Methods of theoretical physics. — New York: McGraw Hill, 1953. — 1061 p.

Received in final form September 17, 2010